Multi-dimensional and Multi-threshold Airframe Damage Region Division Method Based on Correlation Optimization

*CAI Shuyu**, *SHI Tao*, *SHI Lizhong*

College of Aeronautical Engineering, Civil Aviation University of China, Tianjin 300300, P.R. China

(Received 30 June 2020; revised 15 July 2021; accepted 15 September 2021)

Abstract: In order to obtain the image of airframe damage region and provide the input data for aircraft intelligent maintenance, a multi-dimensional and multi-threshold airframe damage region division method based on correlation optimization is proposed. On the basis of airframe damage feature analysis, the multi-dimensional feature entropy is defined to realize the full fusion of multiple feature information of the image, and the division method is extended to multi-threshold to refine the damage division and reduce the impact of the damage adjacent region's morphological changes on the division. Through the correlation parameter optimization algorithm, the problem of low efficiency of multi-dimensional multi-threshold division method is solved. Finally, the proposed method is compared and verified by instances of airframe damage image. The results show that compared with the traditional threshold division method, the damage region divided by the proposed method is complete and accurate, and the boundary is clear and coherent, which can effectively reduce the interference of many factors such as uneven luminance, chromaticity deviation, dirt attachment, image compression, and so on. The correlation optimization algorithm has high efficiency and stable convergence, and can meet the requirements of aircraft intelligent maintenance.

Key words: airframe damage region division; multi-dimensional feature entropy; multi-threshold; correlation optimization; aircraft intelligent maintenance

CLC number: V267 **Document code:** A **Article ID:** 1005-1120(2021)05-0788-12

0 Introduction

With the development of aircraft intelligent maintenance technology, the image processing and modeling of airframe damage has increasingly become an important means of maintenance support. The segmentation of the damage region in the airframe damage image is the basis of this process.

Through analyzing a large number of common local damage of aircraft, such as pit, crack, corrosion, wear and so on, it can be seen that the pixels in the damaged region and the non-damaged region have obvious differences in color, gray level, brightness and other features, and these features are basically similar in the same region. Besides, most of the airframe damage has a certain affected range, which makes the morphology of the damage adjacent region change in different degrees. The existence of the damage transition region has a significant adverse effect on the accurate division of the damage region.

Multi-threshold segmentation method is a typical method to implement the damage region segmentation involving transition region. Numerous theoretical approaches have been proposed by scholars, and solutions have been given for applications in various fields. A multi-threshold image segmentation algorithm was proposed using the Bernstein polynomial to uniformly approximate histogram curve in Ref.[1]. A multilevel image segmentation based on the Tsallis entropy was proposed in Ref.[2]. Ref.[3] introduced multi-threshold image processing into the adaptive object selection. A fuzzy diver-

*Corresponding author, E-mail address: csy0313@163.com.

How to cite this article: CAI Shuyu, SHI Tao, SHI Lizhong. Multi-dimensional and multi-threshold airframe damage region division method based on correlation optimization[J]. Transactions of Nanjing University of Aeronautics and Astronautics, 2021, 38(5):788-799.

http://dx.doi.org/10.16356/j.1005-1120.2021.05.007

gence multi-threshold image segmentation based on the standard deviation was proposed in Ref.[4]. A multi-threshold segmentation based on background subtraction was proposed in Ref.[5] and applied to animal tracking. A gradient and multi-threshold optimization was used to defect detection in Ref.[6]. A multi-threshold automatic segmentation method was proposed in Ref.[7] for field straw mulching detection. The image multi-threshold method was used to characterize the mechanical stability of latex concentrate in Ref.[8]. Ref.[9] presented a stochastic fractal search (SFS) with fuzzy entropy-based multilevel thresholding model for the proper segmentation of color satellite images. These methods represent image features by histogram, information entropy, gradient, divergence and so on, and realize target region division by the multi-threshold method. Most of these methods only consider single-image features such as gray or RGB value, while the appearance of aircraft damage often changes in color, shadow, texture and other aspects at the same time. Because of the single feature representation, some information is lost during damage region segmentation, which affects the segmentation and applicability.

Because of the shortcomings of the threshold segmentation method, such as high computation cost and long computation time, many researches combine the swarm intelligence optimization algorithm to achieve fast threshold optimization. A hybrid bio-inspired learning algorithm proposed in Ref.[10] has an acceptable compromise between its convergence time and its computational cost. Improved artificial bee colony algorithms were proposed in Refs. [11-12] to optimize multi-level threshold image segmentation with lower computational complexity. The modified flower pollination algorithm proposed in Ref.[13] uses a random position vector to improve exploration. The Cuckoo search algorithm in Ref.[14] is improved to search more efficiently in the global range with no gradient information. The modified moth-flame optimization used for multilevel threshold color image segmentation in Ref.[15] has strong exploration ability at the end of iteration. The modified grasshopper algorithm in Ref.[16] can balance the global and local search process through adaptive mechanism. The levy flight trajectory-based salp swarm algorithm was designed for multilevel thresholding image segmentation in Ref.[17], which can maximize the efficiency of resource searches in uncertain environments. In Ref.[18], local search operators were defined to improve the performance of hybrid salp swarm algorithm, combining with fuzzy entropy to realize image multilevel threshold. However, in dealing with multi-dimensional and multi-objective optimization problems, the swarm intelligence algorithm still has some shortcomings, such as low convergence accuracy, poor distribution of solution set, insufficient stability and long calculation time, which cannot meet the requirements of rapid and efficient aircraft intelligent maintenance.

The remainder of the paper is organized as follows. In Section 1 the multi-dimensional and multi-threshold division method based on feature fusion is proposed. The correlation parameter optimization algorithm is designed for the airframe damage region division method in Section 2. Section 3 presents experimental results and analysis. Finally, the conclusions are drawn in Section 4.

1 Multi-dimensional and Multi-threshold Division Method Based on Feature Fusion

1.1 Multi-dimensional feature entropy division method

For a damage image with the size of $M\times N$, multiple feature information functions of pixel (x,y) are defined as $f_1(x,y), f_2(x,y), \cdots, f_n(x,y)$, all of which satisfy $f_i(x,y)\in[0,L-1]$, where $1\leqslant x\leqslant M$, $1\leqslant y\leqslant N$, and L is the feature level of damage image.

There is a n-dimensional feature threshold vector $T=(T_1,T_2,\cdots,T_n)$ divided the pixels of damage image into two categories.

(1) Target class

$\text{Class}_o = \{(x, y) | f_1 \leqslant T_1, f_2 \leqslant T_2, \cdots, f_n \leqslant T_n\}$

(2) Background class

$\text{Class}_b = \{(x, y) | f_1 > T_1, f_2 > T_2, \cdots, f_n > T_n\}$

Let $h_{i_1 i_2 \cdots i_n}$ denote the frequency that the feature function corresponding to any dimension $j (j = 1, 2, \cdots, n)$ satisfies $f_j(x, y) = i_j$, which is abbreviated as $h_{i_{1n}}$. Then the joint probability density is $p_{i_{1n}} = \dfrac{h_{i_{1n}}}{M \times N}$.

The target class feature entropy of the kth-dimensional and T_kth-feature level is defined as

$$H_{ok} = -\sum_{i=0}^{T_k} h_{i_{1n}} \frac{i}{\sum_{j=0}^{T_k} h_{j_{1n}} j} \ln\left(\frac{i}{\sum_{j=0}^{T_k} h_{j_{1n}} j}\right) \tag{1}$$

The background class feature entropy of the kth-dimensional and T_kth-feature level is defined as

$$H_{bk} = -\sum_{i=T_k+1}^{L-1} h_{i_{1n}} \frac{i}{\sum_{j=T_k+1}^{L-1} h_{j_{1n}} j} \ln\left(\frac{i}{\sum_{j=T_k+1}^{L-1} h_{j_{1n}} j}\right) \tag{2}$$

Thus the feature entropy sum of the kth-dimensional and T_kth-feature level is

$$\Phi(T_k) = H_{ok} + H_{bk} \tag{3}$$

The feature entropy sum of target class and background class is

$$\Phi(T) = H_o + H_b = -\sum_{i_1=0}^{T_1}\sum_{i_2=0}^{T_2}\cdots\sum_{i_n=0}^{T_n} p_{oi_{1n}} \ln(p_{oi_{1n}}) - \sum_{i_1=T_1+1}^{L-1}\sum_{i_2=T_2+1}^{L-1}\cdots\sum_{i_n=T_n+1}^{L-1} p_{bi_{1n}} \ln(p_{bi_{1n}}) \tag{4}$$

where

$$p_{oi_{1n}} = \frac{p_{i_{1n}}}{\sum_{i_1=0}^{T_1}\sum_{i_2=0}^{T_2}\cdots\sum_{i_n=0}^{T_n} p_{i_{1n}}}$$

$$p_{bi_{1n}} = \frac{p_{i_{1n}}}{\sum_{i_1=T_1+1}^{L-1}\sum_{i_2=T_2+1}^{L-1}\cdots\sum_{i_n=T_n+1}^{L-1} p_{i_{1n}}}$$

For multi-dimensional feature entropy division method, when the feature entropy sum $\Phi(T)$ is taken as the maximum value, the optimal threshold T^* of overall image segmentation can be obtained.

1.2 Multi-dimensional and multi-threshold division method

Due to the existence of damage transition region, the damage region can be accurately divided by the multi-dimensional and multi-threshold division method.

For the damage image with the size of $M \times N$, assuming that there are mn-dimensional threshold vectors $T_r = (T_{r1}, T_{r2}, \cdots, T_{rn})$, where $r = 1, 2, \cdots, m$, the pixels of the damage image are divided into $m + 1$ categories.

The rth class is $\text{Class}_r = \{(x, y) | T_{r1} < f_1 \leqslant T_{(r+1)1}, \cdots, T_{rn} < f_n \leqslant T_{(r+1)n}\}$.

The rth class feature entropy of the kth-dimension is defined as

$$H_{rk} = -\sum_{i=T_{rk}}^{T_{(r+1)k}} h_{i_{1n}} \frac{i}{\sum_{j=T_{rk}}^{T_{(r+1)k}} h_{j_{1n}} j} \ln\left(\frac{i}{\sum_{j=T_{rk}}^{T_{(r+1)k}} h_{j_{1n}} j}\right) \tag{5}$$

Thus the feature entropy sum of the rth class is

$$\Phi(T_r) = \sum_{k=0}^{n} H_{rk} \tag{6}$$

The characteristic entropy sum of the $R + 1$ classes is

$$\Phi(T_1, T_2, \cdots, T_m) = \sum_{r=0}^{m}\sum_{k=0}^{n} H_{rk} = -\sum_{r=0}^{m}\sum_{k=0}^{n}\sum_{i=T_{rk}}^{T_{(r+1)k}} p_{ri_{1n}} \ln(p_{ri_{1n}}) \tag{7}$$

where $p_{ri_{1n}} = \dfrac{p_{i_{1n}}}{\sum_{i_1=T_{r1}}^{T_{(r+1)1}}\sum_{i_2=T_{r2}}^{T_{(r+1)2}}\cdots\sum_{i_n=T_{rn}}^{T_{(r+1)n}} p_{i_{1n}}}$.

For multi-dimensional and multi-threshold division method, the optimal threshold $(T_1^*, T_2^*, \cdots, T_m^*)$ should meet

$$(T_1^*, T_2^*, \cdots, T_m^*) = \underset{T_1 < T_2 < \cdots < T_m}{\operatorname{argmax}} \Phi(T_1, T_2, \cdots, T_m) \tag{8}$$

For the multi-dimensional and multi-threshold division method based on feature fusion, the color, brightness, texture and other feature information of the damage image are fused to be the judgment basis for damage region division by the definition of multi-dimensional feature entropy. And combined with multi-threshold, it is possible to finely distinguish the complex morphological changes of the damage adjacent regions, reduce the confusion introduced by the damage adjacent regions, and improve the accuracy of damaged region division.

2 Correlation Parameter Optimization Algorithm

In the practical application of damage region segmentation, the definition of multi-dimensional features and the determination of the number of thresholds mostly depend on professional knowledge, which affects the performance of the division method. When the threshold dimension and number increase, the time complexity of the multi-dimensional and multi-threshold division method increases exponentially, which is difficult to meet the rapid and efficient demand of aircraft intelligent maintenance.

In order to solve the computational efficiency problem of the multi-dimensional and multi-threshold division method, the optimization algorithm can be introduced to select the optimal threshold efficiently.

Through the analysis of the method, it can be seen that there are correlations among the multi-dimensional entropy thresholds, which need to be optimized in turn.

For the mn-dimensional feature entropy thresholds, the optimization process is to determine points in mn-dimensional space to satisfy Eq.(8). The process of the correlation parameter optimization algorithm is shown in Fig.1, and the steps are as follows:

Step 1 Initializing the algorithm parameters.

The parameters of the correlation parameter optimization algorithm include the grid size s, the number of the initial threshold (except the first dimension) c_0, the number of the first dimensional initial threshold c_1, the optimization step t, the discrete ratio d, and the cycle times N_c.

Step 2 Gridding the optimization space.

The n-dimensional optimization space is discretized according to the grid size s.

Step 3 Generating the coordinates of initial thresholds.

The initial threshold coordinates are generated randomly according to the association logic: $\text{Class}_r = \left\{(x, y) | T_{r1} < f_1 \leqslant T_{(r+1)1}, \cdots, T_{rn} < f_n \leqslant T_{(r+1)n}\right\}$.

In the first dimension, a certain number (c_1) of values v_{1j} ($j = 1, \cdots, c_1$) are determined randomly within the value range. In the second dimension, for each v_{1j}, the number (c_0) of values v_{2j} are determined randomly between v_{1j} and its maximum, and a total of $c_1 \times c_0$ values are obtained. Similarly, in the ith dimension, for each $v_{(i-1)j}$, the number (c_0) of values v_{ij} are determined randomly between $v_{(i-1)j}$ and its maximum, and a total of $c_1 \times \prod_2^i c_0$ values are obtained. This process continues to the nth dimension so as to generate the number ($c_1 \times \prod_2^n c_0$) of n-dimensional initial thresholds' coordinates ($v_{1j}, v_{2j}, \cdots, v_{nj}$), where $j = 1, 2, \cdots, c_1 \times \prod_2^n c_0$.

Step 4 Calculating the sum of initial feature entropy.

Taking the coordinates of the thresholds as input, the feature entropy Φ_j and the maximum value $\Phi_{\max}$ are calculated according to Eq.(7).

Step 5 Local optimization.

For each threshold coordinate, starting from the first dimension, the feature gradients of 2^n directions are calculated for the current dimension v_{ij}. The direction with the largest feature gradient is selected as the optimization direction of v_{ij}, and taking a unit step t forward to generate a new threshold coordinate. Calculate the feature entropy sum Φ_j' of the new coordinate according to Eq.(7).

Compare the feature entropy sum Φ_j' of the current coordinate with the maximum value $\Phi_{\max}$. If Φ_j' is greater than $\Phi_{\max}$, then continues to take a unit step t forward along the optimization direction, generate a new threshold coordinate and calculate the sum feature entropy. The cycle stops until $\Phi_j' \leqslant \Phi_{\max}$, and the next dimension value of the current threshold coordinate is processed.

For $c_1 \times \prod_2^n c_0$ n-dimensional threshold coordinates, it is needed to complete local optimization,

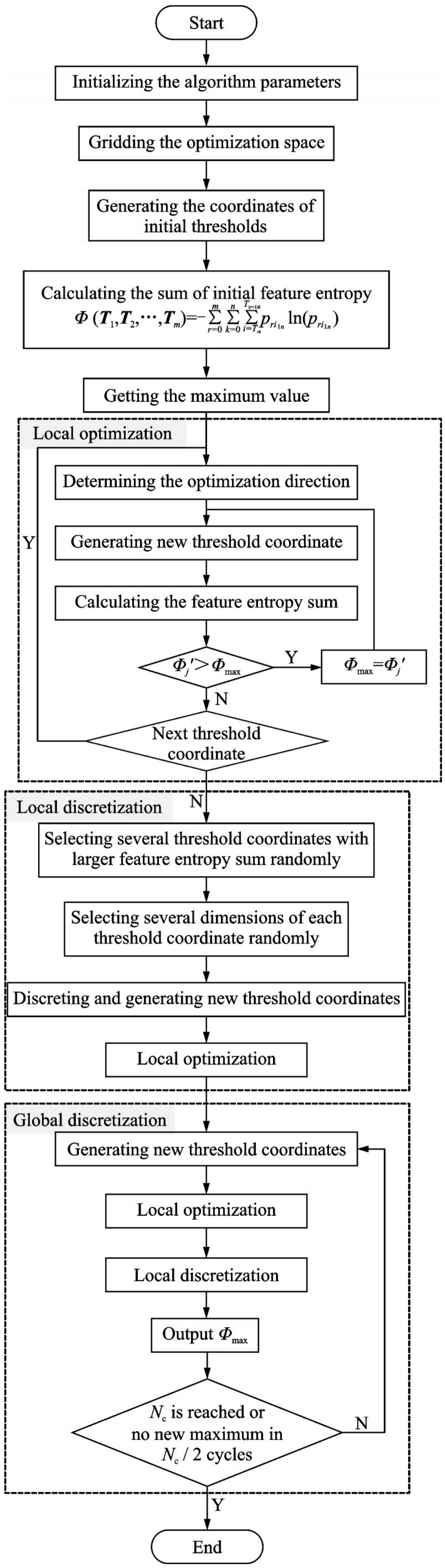

Fig.1 Process of the proposed method

and determine the feature entropy, the maximum value $\Phi_{\max}$ and the corresponding threshold coordinate.

Step 6 Local discretization.

Select several threshold coordinates with the larger feature entropy sum randomly, then select several dimensions of each threshold coordinate randomly. Discrete the selected dimension value of the selected coordinate according to random directions and random distances, then generate new threshold coordinates.

Repeat Step 5.

Step 7 Global discretization.

Calculate global discrete quantity $c_1\times\prod_2^n c_0\times d\%$.

According to Step 3, generate $c_1\times\prod_2^n c_0\times d\%$ new threshold coordinates by global discretization.

Repeat Steps 4, 5 to calculate the feature entropy sum, the maximum value $\Phi'_{\max}$ and the corresponding threshold coordinates of global discrete coordinates.

Compare the global discrete maximum $\Phi'_{\max}$ with the maximum value $\Phi_{\max}$. If the global discrete maximum $\Phi'_{\max}$ is greater than the maximum value $\Phi_{\max}$, $\Phi_{\max}=\Phi'_{\max}$. Repeat Steps 6, 7 until the number of cycles N_c is reached or there is no new maximum in $N_c/2$ cycles.

Step 8 Damage region division.

The damage region image is divided by the threshold coordinate corresponding to the maximum value $\Phi_{\max}$.

The proposed algorithm can be applied to the optimization problem of multiple variables with association relationship. Compared with the traditional optimization algorithm, the association judgment is mostly carried out in the optimization process or after optimization, which will lead to unstable optimization time, ignoring the optimal solution and so on. By defining association rules, the correlation parameter optimization algorithm delimits the effective solution space. On the basis of reducing the necessary optimization space, it avoids the invalid operation that does not conform to the association logic rules, and improves the calculation efficiency. Therefore, the algorithm takes association rules as the premise of random location, which can accelerate the optimization process and solve the complex problem of multivariable association optimization within $O(n\log n)$ time complexity. Meanwhile, the local discrete process and global discrete process are set to improve the global search ability of the algorithm and avoid the sensitivity of the initial value.

3 Experimental Results and Analysis

Six Instances 1—6 are given to verify the multi-dimensional and multi-threshold airframe damage region division method based on correlation optimization. The images of Instances 1—6, i.e., cracks in airframe surface, bird strike damage at wing leading edge, skin surface patch cracks, lightning ablation, exfoliation of skin paint layer, and pit at vertical tail leading edge, are shown in Fig.2, and the image features of each instance are shown in Table 1.

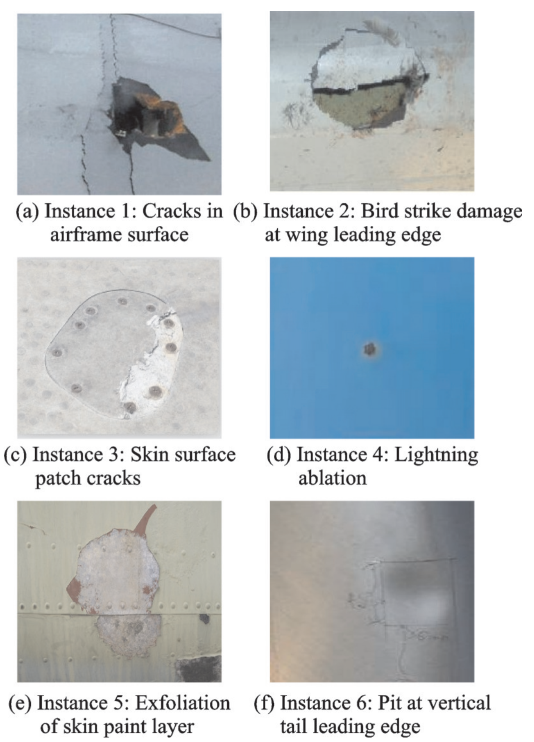

(a) Instance 1: Cracks in airframe surface (b) Instance 2: Bird strike damage at wing leading edge (c) Instance 3: Skin surface patch cracks (d) Instance 4: Lightning ablation (e) Instance 5: Exfoliation of skin paint layer (f) Instance 6: Pit at vertical tail leading edge

Fig.2 Airframe damage image instances

3.1 Division effect verification

In order to verify the division quality of the proposed method, the 1-D single-threshold division method is selected for comparison. In the selected method, the gray entropy is used to divide the damage region of instances. In the method, two feature information functions $f_1(x,y)$, $f_2(x,y)$ are used. $f_1(x,y)$ is the chromaticity value at the pixel (x,y) and $f_2(x,y)$ is the maximum luminance difference in the neighborhood. The calculation results are shown in Tables 2, 3, and the result images of each instance are shown in Fig.3.

Through the verification results, it can be seen

Table 1 Instance image features

Instance	Damage region	Damage boundary	Adjacent region
1	Obvious	Clear	Small
2	Obvious, complicated with hollow structure	Bird strike stains around	Not exist
3	Obvious	Clear	Obvious morphological changes
4	Obvious, concentrated	Clear	Small
5	Obvious	Clear	Obvious morphological changes
6	Not obvious, luminance changes	Not obvious	Interference of manual marking

Table 2 Calculation results based on 1-D single-threshold division method

Instance	Gray threshold	Gray entropy	Running time/ms
1	163	22.159 1	141
2	175	19.510 8	125
3	201	20.235 3	281
4	141	19.983 3	404
5	162	22.291 5	440
6	138	19.352 1	284

Table 3 Calculation results based on the proposed method

Instance	Feature value				Feature entropy Φ	Running time/ms
	T_{11}	T_{12}	T_{21}	T_{22}		
1	45	4	109	45	17.487 8	594
2	95	5	158	54	16.644 7	796
3	130	4	203	30	16.234 1	818
4	69	4	110	45	8.412 6	390
5	105	1	149	35	17.479 5	734
6	104	3	145	65	12.027 6	603

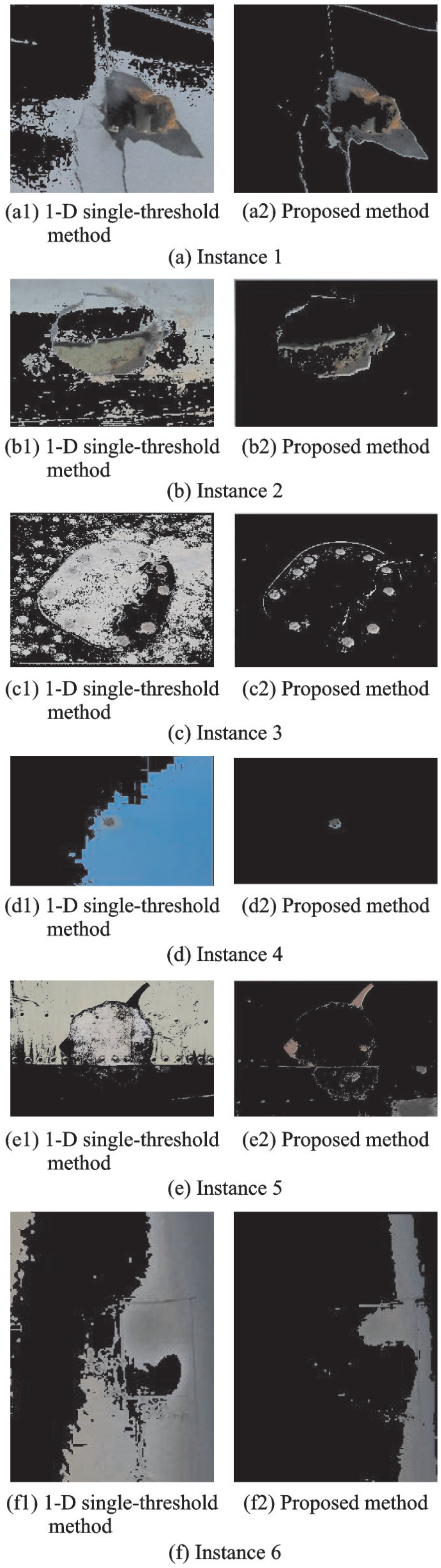

Fig.3 Damage region division images

that the operation speed of the 1-D single-threshold division method is faster. The computation of both methods can be completed in milliseconds. The operation speed of the proposed method is acceptable. However, the division effect of the 1-D single-threshold division method is not ideal. In the original image of Instance 1, the boundary of damage region is clear, and the chromaticity contrast between the damage region and non-damage region is obvious. There are several obvious cracks, and the damage adjacent region is small. After the division by the 1-D single-threshold method, lots of non-damage regions still exist, and crack damage could not be divided accurately. The division result of the proposed method shows that the damage region is accurately divided with intact boundary, clear divided crack, good consistency and less noise. The non-damage region introduced by 1-D single-threshold method is excluded.

In the original image of Instance 2, the damage is composed of two parts, namely the skin fragmentation of wing leading edge and the peeling off of skin due to bird strike. The damage form is complicated with hollow damage structure. Adjacent region usually does not exist in the foreign object damage, but some bird strike stains and a few feathers around the damage region of the image have some influence on the damage region division. After the division by the 1-D single-threshold method, the information loss of damage region is serious, and lots of non-damage regions are introduced. The division result of the proposed method shows that the damage region is completely divided with few noise. The boundary of the two damage parts is clear. Obviously, the bird strike dirt and the complex structure have little influence on damage region division.

In the original image of Instance 3, the boundary of patch cracks is obvious, but a large range of pitting corrosion appears on the skin of damage adjacent region, which greatly interferes the damage region division. The division based on the 1-D single-threshold method could not distinguish the noise of adjacent regions, and is poor in division effect. The division result of the proposed method shows that the damage region is clear, the details of the rivets and fractures in the damage region are obvious and the boundary is complete. A little noise is introduced by the adjacent region.

In the original image of Instance 4, the ablation region is concentrated, the adjacent region is small, and the chromaticity contrast of non-damaged region is obvious. However, the indiscernible luminance change introduced in the image acquisition process and the information compression in the image transmission process make adverse effect on division, so that a large number of non-damage regions are introduced into the division results of the 1-D single-threshold method. However, the divided ablation region of the proposed method is clear and its boundary is complete. The luminance change and information compression of original image do not interfere with the division. The non-damage region introduced by 1-D single-threshold method is excluded.

Instance 5 is the image of exfoliation of skin paint layer, which contains many damage regions with clear boundary and slight morphology change around damage. But dust adhering to the lower part of the skin overlapping structure greatly influences the division. The damage region divided by the 1-D single-threshold method could not be divided completely and lots of non-damage regions are introduced. Through the proposed method, many damage regions in the image are divided clearly, and the boundary is coherent. It avoids the interference of dust adhering to the lower part of skin overlapping structure, and eliminates the non-damage region existed in the 1-D single-threshold division result.

The original image of Instance 6 has certain luminance changes at the pit, the damage region has no obvious boundary, and the interference of manual marking is existed. The damage region divided by the 1-D single-threshold method is not accurate, and lots of non-damage regions with similar color are introduced. Through the proposed method, the complete pit damage region is obtained, and the interference of influence change and the color similarity to the division is reduced. However, due to the obvious manual marking in the original image, there is still a small amount of marking information in the divided image of the damage region.

It can be seen that in the actual aircraft inspection and maintenance, the acquired damage image may be affected by the external factors such as uneven luminance, chromaticity deviation, dust adhesion, image compression and so on. For the morphological diversity of damage area and adjacent area, the proposed method eliminates these interferences, and the division effect is better.

3.2 Optimization effect verification

In order to verify the effect of the correlation parameter optimization algorithm, the bacterial foraging optimization (BFO) algorithm is selected for comparative analysis. As shown in Table 4, in order to ensure the fairness of algorithm comparison, the corresponding parameter settings of the two algorithms are consistent. The results of BFO algorithm are shown in Table 5.

Table 4 Parameter setting of optimization algorithm

Parameter	Value	
	Proposed algorithm	BFO algorithm
Grid size s	1	
Number of the 1st dimensional initial threshold c_1	5	10
Number of the initial threshold (Except the 1st dimension) c_0	2	10
Optimization step t	2	2
Discrete ratio d	0.25	0.25
Cycle times N_c	20	20

Table 5 Calculation results based on the BFO algorithm

Instance	Number of optimization points	Proportion of invalid points/%	Running time/ms
1	580	94.83	1 564
2	672	94.94	1 437
3	717	79.08	1 444
4	312	93.59	943
5	573	89.18	1 598
6	394	94.42	1 284

It can be seen that a large number of optimization points generated by the BFO algorithm do not conform to the association logic. In the BFO optimization process of each instance, the proportion of invalid optimization points reaches more than 75%. And there are also a certain number of edge overflow points. These invalid points cause a waste of computing resources and time.

From Tables 3, 5, it can be seen that the proposed algorithm has certain advantages in computing time compared with the BFO algorithm. The proposed algorithm takes the defined association rules as the basis for the generation of optimization points, which avoids the occurrence of logical inefficiency and improves the calculation efficiency.

In the following, ten groups of operations are performed on each instance to further verify the correlation parameter optimization algorithm. The convergence processes of feature entropy sum are shown in Fig.4. The deviation of feature entropy sum of each group is shown in Table 6.

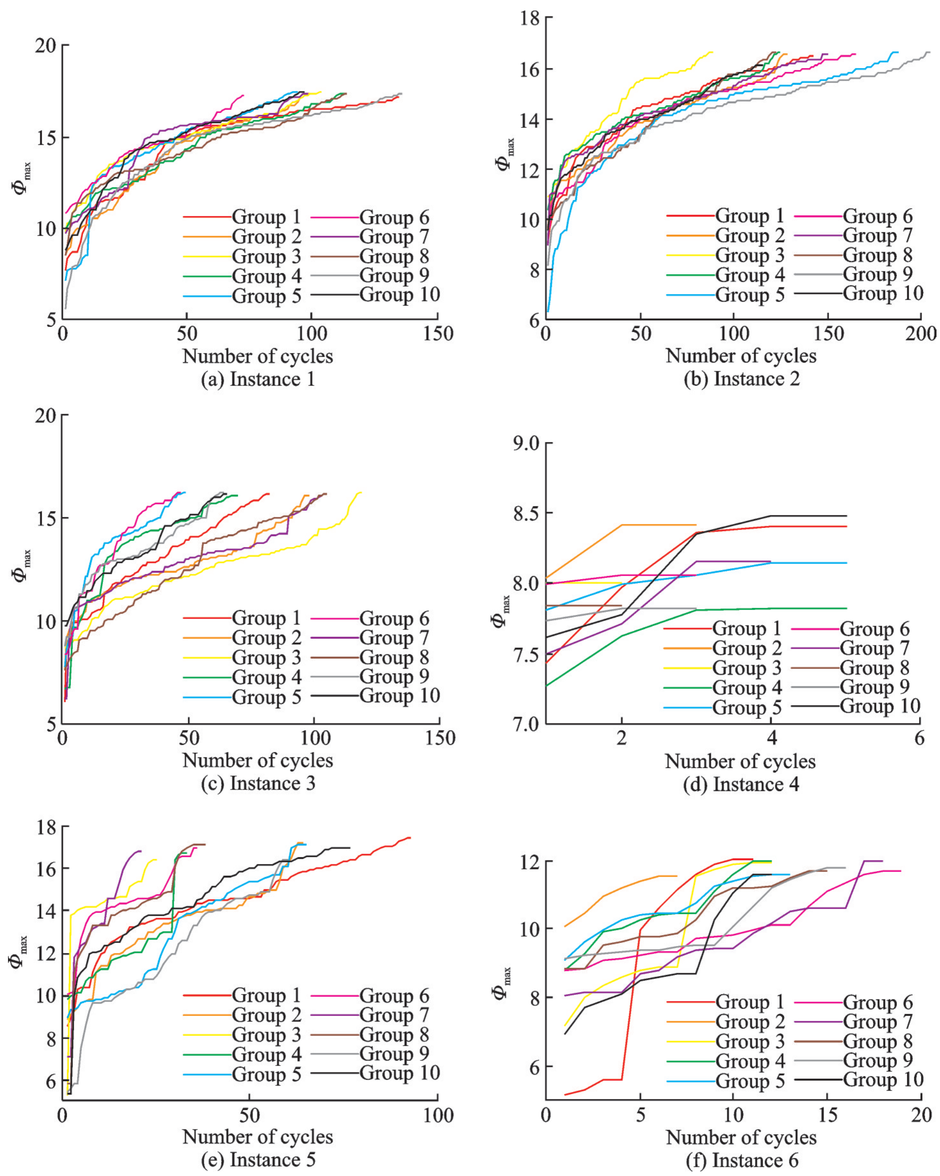

Fig.4 Convergence process of ten groups

As can be seen from Fig.4 and Table 6, for Instances 1—3, the information quantity of the image is rich, which can provide sufficient data support for the optimization algorithm. It can ensure the continuous optimization of the feature entropy of each link of the algorithm. The convergence effects of ten groups are stable, and the group deviation of feature entropy is small. The image of Instance 4 has low information quantity and large background area, which affects the discretization in the optimization process and increases the probability that the points generated in the local discretization and global discretization process fall into the background area. However, the background area with uniform features and large region cannot effectively support the local optimization of points, and it is difficult to further optimize the points after falling into the background area, which may affect the optimization results. From the convergence effect of ten groups of operations, it can be seen that there is a certain deviation between the feature entropy groups. The image information quantity of Instance 5 is rich, but the damage adjacent region is not significant. The verification of the proposed method uses double thresholds, which can avoid the influence of the damage adjacent region while dividing the damage region. But there is no obvious adjacent region in Instance 5, the double thresholds subdivide the damage area, which makes the local optimization continue and makes the optimization range be limit in the damage area. It will affect the convergence result and cause some fluctuation. The Instance 6 is pit damage, the image chroma is single, but there is a certain brightness change. In the proposed method, the 2nd dimension feature entropy is the maximum luminance difference in the neighborhood. The luminance change can be perceived in the optimization process, which can provide information support for optimization. The convergence effects of ten groups of operations are relatively stable, and the group deviation of characteristic entropy is relatively small.

In Table 6, the calculation results of each instance are statistically tested. Under the significance level $\alpha = 0.05$, suppose $H_0: \mu \leqslant \mu_0$, the total number of samples is $n = 10$, the critical point is $t_{0.05}(9) = 1.833\,1$, and calculate the test statistic $t = \dfrac{\overline{X} - \mu_0}{S/\sqrt{n}}$, where $\overline{X}$ is the arithmetic mean of the calculation results and S the standard deviation of the calculation results. It can be seen that the test statistics of each instance are less than the critical point, and H_0 is accepted. That is to say, for each instance, the average error of the proposed method is at a low level.

Table 6 Calculation results based on the proposed method

Instance	Group deviation / %										μ_0	Test statistics t
	1	2	3	4	5	6	7	8	9	10		
1	1.84	0.91	0.37	0.68	0.00	1.19	0.78	0.78	0.87	0.05	0.5	1.446 2
2	1.08	0.47	0.02	0.29	0.08	0.58	0.35	0.28	0.00	3.10	0.1	1.792 6
3	0.66	0.83	0.00	0.91	0.24	0.30	0.68	0.39	0.17	0.34	0.3	1.596 2
4	0.17	0.00	4.90	7.05	3.29	4.31	3.12	6.74	7.09	4.93	2.7	1.790 8
5	0.00	1.35	6.07	4.04	1.80	2.76	3.58	1.98	6.06	2.62	1.9	1.815 9
6	0.00	3.84	0.97	0.50	3.57	2.96	0.40	2.81	1.86	3.44	1.2	1.799 4

4 Conclusions

Based on the definition of multi-dimensional feature entropy, introducing the idea of multi-threshold segmentation and designing the optimization algorithm for correlation parameters, the multi-dimensional and multi-threshold airframe damage region division method based on correlation optimization is proposed. The method is verified by various airframe structure damage images. The verification results show that:

(1) From the perspective of the operation speed, the operation process of the proposed method can be completed in the method within millisecond scope, and with low time complexity.

(2) From the perspective of division quality, compared with the traditional 1-D single threshold division method, the damage region obtained by this method has high accuracy, consistent and complete boundary. It can effectively divide cracks, pits, foreign object damage and other common structural damage forms of the airframe with less noise. For the interference factor introduced in the image acquisition process, it has good anti-interference effect, and the overall division result is better than the traditional method.

(3) From the perspective of optimization effect, the rapid convergence could be achieved and the optimal solution of convergence is stable.

(4) From the perspective of applicability, the proposed method is suitable for the processing of complex damage images with adjacent damage re-

gions or high information quantity. For the simple damage image with large range of low information quantity area, the proposed method may subdivide the region and introduce errors.

Therefore, the proposed method can rapidly and effectively achieve the division of airframe damage region, and provide data foundation and technical support for the airplane structure damage model reconstruction, airplane structure damage analysis and repair design.

References

[1] WEI Yanjun, FENG Boqin, WU Weiguo. Multi-threshold algorithm about image segmentation based on polynomial uniform approximation[J]. Journal on Communications, 2016,36(10): 56-64.

[2] RODRIGUES P S, WACHS-LOPES G A, ERSMANN H R, et al. Improving a firefly meta-heuristic for multilevel image segmentation using Tsallis entropy[J]. Pattern Analysis and Applications, 2017, 20(1): 1-20.

[3] BOGACHEV M I, MARKELOV O A, VOLKOV V Y. Adaptive object selection based on multi-threshold image processing[C]//Proceedings of Wave Electronics and Its Application in Information and Telecommunication Systems(WECONF). [S.l.]: IEEE, 2019: 1-5.

[4] YANG M, LEI B, SHI L N, at al. Fuzzy divergence multi-threshold image segmentation based on standard deviation[J]. Computer Applications and Software, 2020, 37(5): 219-225.

[5] SURENDAR E, THOMAS V M, POSONIA A M. Animal tracking using background subtraction on multi threshold segmentation[C]//Proceedings of International Conference on Circuit, Power and Computing Technologies(ICCPCT). Nagercoil: IEEE, 2016: 1-6.

[6] GAO Yin, LI Jun. Defect detection algorithm based on gradient and multithreshold optimization[C]//Proceedings of 2015 IEEE International Conference on Information and Automation (ICIA). Lijiang: IEEE, 2015: 1393-1396.

[7] LIU Yuanyuan, WANG Yueyong, YU Haiye, et al. Detection of straw coverage rate based on multi-threshold image segmentation algorithm[J]. Transactions of the Chinese Society for Agricultural Machinery, 2018, 49(12): 34-42,62.

[8] LAI W K, PHOON Z H, CHEW K H, et al. Image multi-thresholding to characterize the mechanical stability of rubber latex concentrate[C]//Proceedings of 2016 International Conference on Digital Image Computing: Techniques and Applications(DICTA). Gold Coast: IEEE, 2016: 1-8.

[9] DHAL K G, RAY S, DAS A, et al. Fuzzy multi-level color satellite image segmentation using nature-inspired optimizers: A comparative study[J]. Journal of the Indian Society of Remote Sensing, 2019, 47(4): 1391-1415.

[10] DEHSHIBI M M, SOURIZARI M, FAZLALI M, et al. A hybrid bio-inspired learning algorithm for image segmentation using multilevel thresholding[J]. Multimedia Tools & Applications, 2017, 76(14): 15951-15986.

[11] MA Lianbo, WANG Xingwei, SHEN Hai, et al. A novel artificial bee colony optimiser with dynamic population size for multi-level threshold image segmentation[J]. International Journal of Bio Inspired Computation, 2019, 13(1): 32-44.

[12] EWEES A A, ELAZIZ M A, AL-QANESS M A A, et al. Improved artificial bee colony using sine-cosine algorithm for multi-level thresholding image segmentation[J]. IEEE Access, 2020,8: 26304-26315.

[13] SHEN Liang, FAN Chongyi, HUANG Xiaotao. Multi-level image thresholding using modified flower pollination algorithm[J]. IEEE Access, 2018, 6: 30508-30519.

[14] WU Lushen, CHENG Wei, HU Yun. Image segmentation of multilevel threshold based on improved cuckoo search algorithm[J]. Journal of Jilin University (Engineering and Technology Edition), 2020,51(1): 358-369.

[15] JIA Heming, MA Jun, SONG Wenlong. Multilevel thresholding segmentation for color image using modified moth-flame optimization[J]. IEEE Access, 2019, 7: 44097-44134.

[16] LIANG Hongnan, JIA Heming, XING Zhikai, et al. Modified grasshopper algorithm based multilevel thresholding for color image segmentation[J]. IEEE Access, 2019, 7: 11258-11295.

[17] XING Zhikai, JIA Heming, SONG Wenlong. Levy flight trajectory-based salp swarm algorithm for multilevel thresholding image segmentation[J]. Acta Automatica Sinica, 2021, 47(2): 363-377.

[18] ALWEIFALI H S N, ELAZIZ M A, AL-QANESS M A A, et al. A multilevel image thresholding based on hybrid salp swarm algorithm and fuzzy entropy[J]. IEEE Access, 2019, 7: 181405-181422.

Acknowledgement The work was supported by the Aeronautical Science Foundation of China (No.20151067003).

Author Ms. **CAI Shuyu** received the B.S. degree in computer science and technology from Shandong University (SDU) in 2007 and the M.S. degree in man-machine and environmental engineering from Civil Aviation University of China (CAUC) in 2010. In May 2010, she joined College of Aeronautical Engineering, CAUC, Tianjin, China. Now she is engaged in the research of aircraft predictive maintenance and domestic civil aircraft operation support. Her research interest includes aircraft performance predictive monitoring and aircraft damage intelligent detection.

Author contributions Ms. **CAI Shuyu** conceived and supervised the study, revised and modified the manuscript. Mr. **SHI Tao** wrote the manuscript. Mr. **SHI Lizhong** contributed to the tests. All authors commented on the manuscript draft and approved the submission.

Competing interests The authors declare no competing interests.

(Production Editor: SUN Jing)

基于关联优化的多维多阈值机体损伤区域划分

蔡舒妤，史　涛，师利中

（中国民航大学航空工程学院，天津 300300，中国）

摘要：为了快速获取机体损伤区域图像，为飞机智能维修提供数据输入，提出了一种基于关联优化的多维多阈值机体损伤区域划分方法。在机体损伤特征分析的基础上，定义了多维特征熵以充分融合损伤图像多样化特征信息。通过设计多阈值损伤区域划分方法，细化了损伤区域，减少了损伤邻域形态变化对划分效果的影响。使用关联参数优化算法解决了多维多阈值划分方法效率低下的问题。最后，以机身损伤图像为例，对该方法进行了对比和验证。结果表明，与传统的阈值划分方法相比，该方法划分的损伤区域准确完整、边界清晰，可以有效地减少亮度不均匀、色度偏差、污垢附着及图像压缩等诸多因素的干扰。关联优化算法效率高且收敛稳定，能够满足飞机智能维修的要求。

关键词：机体损伤区域划分；多维特征熵；多阈值；关联优化；航空器智能维修